

# Ensemble Kalman Inversion for General Likelihoods

Samuel Duffield     Sumeetpal S. Singh  
University of Cambridge

July 1, 2022

## Abstract

Ensemble Kalman inversion represents a powerful technique for inference in statistical models with likelihoods of the form  $y | x \sim \mathbf{N}(y | \mathcal{H}(x), \mathbf{R})$  where the forward operator  $\mathcal{H}$  and covariance  $\mathbf{R}$  are known. In this article, we generalise ensemble Kalman inversion to models with general likelihoods,  $y | x \sim p(y | x)$  where the likelihood can be sampled from, but its density not necessarily evaluated. We examine the ensemble Kalman performance for both optimisation and uncertainty quantification against fully adaptive approximate Bayesian computation techniques.

## 1 Introduction

The *ensemble Kalman filter* [7] represents a popular tool for online inference in high-dimensional spatio-temporal models - most commonly in meteorological applications. More recently, these techniques have been adapted for offline inference in static Bayesian inference models of the form

$$x \sim p(x), \quad y | x \sim \mathbf{N}(y | \mathcal{H}(x), \mathbf{R}), \quad (1)$$

where  $p(x)$  is a prior distribution,  $\mathcal{H}$  a deterministic forward operator and  $\mathbf{R}$  a noise covariance matrix which we assume are all known. The use of ensemble Kalman techniques for offline Bayesian models is known as *ensemble Kalman inversion* [13].

Ensemble Kalman techniques are known to be asymptotically biased, outside of fully linear Gaussian problems. They have however been used with great success in complex problems often in dimensions far exceeding the number of particles [18]. For this reason, they have remained the method of choice for very high-dimensional state-space models where asymptotically unbiased methods such as particle filters suffer a prohibitive curse of dimensionality [19], as well as becoming increasingly popular in offline Bayesian models (1) where the forward operator may be extremely expensive, [21].

Additionally, the field of *approximate Bayesian computation* (ABC) tackles general Bayesian models

$$x \sim p(x), \quad y | x \sim p(y | x), \quad (2)$$

where the density of the likelihood function  $p(y | x)$  cannot be evaluated or at least cannot be evaluated within a reasonable computational budget. ABC techniques instead rely on the ability to efficiently simulate synthetic data from the likelihood for a given value of the parameter

$$y^{(i)} \sim p(y | x^{(i)}).$$

Simulated data can then be compared to the true observed data and subsequently only parameter values that have generated data sufficiently *close* to the true data are retained. The resulting samples are asymptotically biased, however this bias is quantifiable and controllable. For a relatively recent, thorough review of ABC techniques, see [2].

**The key contribution of this work is to generalise ensemble Kalman inversion to general likelihoods  $p(y | x)$  as opposed to the restrictive additive Gaussian setting  $p(y | x) = \mathbf{N}(y | \mathcal{H}(x), \mathbf{R})$ .** In doing so, we re-frame ensemble Kalman inversion within the context of approximate Bayesian computation and examine numerically the difference between the approaches.

The rest of the letter is structured as follows. Section 2 describes the historical development of the existing ensemble Kalman techniques. We then present our novel generalisation of ensemble Kalman inversion in Section 3 before examining its performance numerically for both optimisation and uncertainty quantification in Section 4. Section 5 concludes and discusses future work.

---

S. Duffield is supported by the UK Engineering and Physical Sciences Research Council (EPSRC) doctoral training award  
Contact: sddd2@cam.ac.uk, sss40@cam.ac.uk

## 2 Ensemble Kalman Approach

Ensemble Kalman techniques were first introduced [7] for generating online Monte Carlo approximations for state-space models.

For simplicity consider the offline setting in (1) where the likelihood takes the form  $p(y | x) = \mathbf{N}(y | \mathcal{H}(x), \mathbf{R})$ . Then a single update step of the ensemble Kalman filter as described in [8] takes the form

$$\begin{aligned} x_1^{(i)} &= x_0^{(i)} + C_0^{x\mathbf{H}} (C_0^{\mathbf{H}\mathbf{H}} + \mathbf{R})^{-1} (y - \mathcal{H}(x_0^{(i)}) - \eta^{(i)}), \\ \eta^{(i)} &\sim \mathbf{N}(\eta | 0, \mathbf{R}), \end{aligned} \quad (3)$$

with prior samples  $x_0^{(i)} \sim p(x)$ , empirical covariance matrices

$$\begin{aligned} C_0^{x\mathbf{H}} &= \frac{1}{N-1} \sum_{i=1}^N (x_0^{(i)} - \bar{x}_0)(\mathcal{H}(x_0^{(i)}) - \bar{\mathcal{H}}(x_0))^T, \\ \hat{C}_0^{\mathbf{H}\mathbf{H}} &= \frac{1}{N-1} \sum_{i=1}^N (\mathcal{H}(x_0^{(i)}) - \bar{\mathcal{H}}(x_0))(\mathcal{H}(x_0^{(i)}) - \bar{\mathcal{H}}(x_0))^T, \end{aligned} \quad (4)$$

and empirical means  $\bar{x}_0 = \frac{1}{N} \sum_{i=1}^N x_0^{(i)}$  and  $\bar{\mathcal{H}}(x_0) = \frac{1}{N} \sum_{i=1}^N \mathcal{H}(x_0^{(i)})$ .

This ensemble Kalman update is asymptotically unbiased in the special case of Gaussian prior and linear Gaussian likelihood

$$p(x) = \mathbf{N}(x | m, \mathbf{Q}), \quad (5a)$$

$$p(y | x) = \mathbf{N}(y | \mathbf{H}x, \mathbf{R}), \quad (5b)$$

$$\implies p(x, y) = \mathbf{N} \left( \begin{pmatrix} m \\ \mathbf{H}m \end{pmatrix}, \begin{pmatrix} \mathbf{Q} & \mathbf{Q}\mathbf{H}^T \\ \mathbf{H}\mathbf{Q} & \mathbf{H}\mathbf{Q}\mathbf{H}^T + \mathbf{R} \end{pmatrix} \right), \quad (5c)$$

with analytically tractable posterior

$$p(x | y) = \mathcal{N}(m^y, \mathbf{Q}^y),$$

$$m^y = m + \mathbf{Q}\mathbf{H}^T (\mathbf{H}\mathbf{Q}\mathbf{H}^T + \mathbf{R})^{-1} (y - \mathbf{H}m), \quad (6a)$$

$$\mathbf{Q}^y = \mathbf{Q} - \mathbf{Q}\mathbf{H}^T (\mathbf{H}\mathbf{Q}\mathbf{H}^T + \mathbf{R})^{-1} \mathbf{H}\mathbf{Q}. \quad (6b)$$

with  $x \in \mathbb{R}^{d_x}$  and  $y \in \mathbb{R}^{d_y}$ . The exact solution to the linear model (5) is the posterior distribution (6) and represents an application of *Kalman inversion*.

Outside of this special linear Gaussian case, the ensemble Kalman update (3) is known to be asymptotically biased. There is however, a vast amount of empirical evidence demonstrating stability in a variety of complex non-linear state-space models with a very small number of particles, e.g. [9], [20]. In our view, this summarises the ensemble Kalman paradigm:

**Asymptotically unbiased in the linear Gaussian case, otherwise biased but empirically stable.**

Where the term *empirically stable* represents the ability of the ensemble of particles to cover the true underlying value of the state without degenerating to a single particle. Naturally, the acceptance of a bias induced by this paradigm could be extreme in some problems, however as mentioned, there is still very much a practical desire for these numerically efficient but biased methods.

For non-Gaussian priors and non-linear Gaussian likelihoods (2), the distribution of particles from a single step ensemble Kalman update may be quite different from the true posterior. However, as introduced in [13], by iterating the ensemble Kalman update in (3) one can still generate a series of informative particles. This idea was refined in [12] to be more in line with the tempered likelihood approach of SMC samplers [5, 15]. This iterative ensemble Kalman approach is termed *ensemble Kalman inversion* and a single iterate takes the form

$$\begin{aligned} x_\ell^{(i)} &= x_{\ell-1}^{(i)} + C_{\ell-1}^{x\mathbf{H}} (C_{\ell-1}^{\mathbf{H}\mathbf{H}} + h_\ell^{-1}\mathbf{R})^{-1} (y - \mathcal{H}(x_{\ell-1}^{(i)}) - \eta_\ell^{(i)}), \\ \eta_\ell^{(i)} &\sim \mathbf{N}(\eta_\ell | 0, h_\ell^{-1}\mathbf{R}). \end{aligned} \quad (7)$$

where  $C_{\ell-1}^{x\mathbf{H}}$  and  $C_{\ell-1}^{\mathbf{H}\mathbf{H}}$  are as in (4) applied to the particles  $\{x_{\ell-1}^{(i)}\}_{i=1}^N$ . The parameter  $h_\ell^{-1}$  can be considered a stepsize parameter or equally  $h_\ell$  as an incremental inverse temperature parameter. In the fully linear Gaussian

case (5), the particles  $\{x_\ell^{(i)}\}_{i=1}^N$  at each step are asymptotically unbiased for a tempered version of the posterior

$$\begin{aligned} p_\ell(x) &\propto p(x)p(y|x)^{\lambda_\ell} \\ &= \mathcal{N}(m_\ell, \mathbf{Q}_\ell), \\ m_\ell &= m + \mathbf{Q}\mathbf{H}^\top (\mathbf{H}\mathbf{Q}\mathbf{H}^\top + \lambda_\ell^{-1}\mathbf{R})^{-1} (y - \mathbf{H}m), \end{aligned} \quad (8a)$$

$$\mathbf{Q}_\ell = \mathbf{Q} - \mathbf{Q}\mathbf{H}^\top (\mathbf{H}\mathbf{Q}\mathbf{H}^\top + \lambda_\ell^{-1}\mathbf{R})^{-1} \mathbf{H}\mathbf{Q}, \quad (8b)$$

where  $\lambda_\ell = \sum_{r=1}^\ell h_r$  is the inverse temperature. The tempered posterior can also be defined iteratively

$$m_\ell = m_{\ell-1} + \mathbf{Q}_{\ell-1}\mathbf{H}^\top (\mathbf{H}\mathbf{Q}_{\ell-1}\mathbf{H}^\top + h_\ell^{-1}\mathbf{R})^{-1} (y - \mathbf{H}m_{\ell-1}), \quad (9a)$$

$$\mathbf{Q}_\ell = \mathbf{Q}_{\ell-1} - \mathbf{Q}_{\ell-1}\mathbf{H}^\top (\mathbf{H}\mathbf{Q}_{\ell-1}\mathbf{H}^\top + h_\ell^{-1}\mathbf{R})^{-1} \mathbf{H}\mathbf{Q}_{\ell-1}, \quad (9b)$$

Thus, we can iterate  $L$  steps with stepsizes such that  $\lambda_L = \sum_{r=1}^L h_r = 1$  and obtain particles  $\{x_L^{(i)}\}_{i=1}^N$  that are asymptotically unbiased for the true posterior in the linear Gaussian case.

Iterating until  $\lambda_L = 1$  is only one possible stopping criterion, another common approach is to adopt an optimisation style stopping criterion, for example [12] suggest termination when the average of the forward operations  $\bar{\mathcal{H}}(x_L)$  is suitably close the true data, i.e. when  $(y - \bar{\mathcal{H}}(x_L))^\top \mathbf{R}^{-1} (y - \bar{\mathcal{H}}(x_L)) < \tau$  for some stopping parameter  $\tau$ .

### 3 Generalised Ensemble Kalman Inversion

In this section, we generalise ensemble Kalman inversion to the case where data is generated according to any likelihood  $p(y|x)$  rather than the setting described in Section 2 which is restricted to likelihoods of the form  $\mathbf{N}(y|\mathcal{H}(x), \mathbf{R})$ . The resulting algorithm only requires samples from the prior  $p(x)$  and the ability to simulate from the likelihood  $p(y|x)$  for a given  $x$ , as in approximate Bayesian computation. The final particle approximation is asymptotically biased for the true posterior with the exception of the fully linear Gaussian case (5) and therefore faithful to the ensemble Kalman paradigm.

#### 3.1 General Likelihoods

In this more general case, we can no longer form the empirical covariance matrices in (4) as we do not have access to the deterministic  $\mathcal{H}$ . Instead we can form

$$\mathbf{C}_\ell^{xx} = \frac{1}{N-1} \sum_{i=1}^N (x_\ell^{(i)} - \bar{x}_\ell)(x_\ell^{(i)} - \bar{x}_\ell)^\top, \quad (10a)$$

$$\mathbf{C}_\ell^{xy} = \frac{1}{N-1} \sum_{i=1}^N (x_\ell^{(i)} - \bar{x}_\ell)(y_\ell^{(i)} - \bar{y}_\ell)^\top, \quad (10b)$$

$$\mathbf{C}_\ell^{yy} = \frac{1}{N-1} \sum_{i=1}^N (y_\ell^{(i)} - \bar{y}_\ell)(y_\ell^{(i)} - \bar{y}_\ell)^\top, \quad (10c)$$

and  $\mathbf{C}_\ell^{yx} = \mathbf{C}_\ell^{xy}^\top$  with simulated data  $y_\ell^{(i)} \sim p(\cdot | x_\ell^{(i)})$ .

In the fully linear Gaussian case (5) or rather the tempered version (8, 9) we have  $\mathbf{C}_\ell^{xy} \rightarrow \mathbf{H}\mathbf{Q}_\ell$  and  $\mathbf{C}_\ell^{yy} \rightarrow \mathbf{H}\mathbf{Q}_\ell\mathbf{H}^\top + \mathbf{R}$ . We now note that we can also calculate

$$\mathbf{C}_\ell^{y|x} = \mathbf{C}_\ell^{yy} - \mathbf{C}_\ell^{yx} \mathbf{C}_\ell^{xx}^{-1} \mathbf{C}_\ell^{xy}, \quad (11)$$

and observe that in the linear Gaussian case

$$\begin{aligned} \mathbf{C}_\ell^{y|x} &\rightarrow (\mathbf{H}\mathbf{Q}_{\ell-1}\mathbf{H}^\top + \mathbf{R}) - (\mathbf{H}\mathbf{Q}_{\ell-1})\mathbf{Q}_{\ell-1}^{-1}(\mathbf{Q}_{\ell-1}\mathbf{H}^\top), \\ &= \mathbf{R}. \end{aligned}$$

Thus we can use the particles to approximate the noise covariance of the likelihood empirically.

We therefore adjust the tempered ensemble Kalman iteration (7) to the following

$$\begin{aligned} x_\ell^{(i)} &= x_{\ell-1}^{(i)} + \mathbf{C}_{\ell-1}^{xy} \left( \mathbf{C}_{\ell-1}^{yy} + (h_\ell^{-1} - 1)\mathbf{C}_{\ell-1}^{y|x} \right)^{-1} \left( y - y_{\ell-1}^{(i)} - \eta_\ell^{(i)} \right), \\ y_{\ell-1}^{(i)} &\sim p(y_{\ell-1} | x_{\ell-1}^{(i)}), \\ \eta_\ell^{(i)} &\sim \mathbf{N}(\eta | 0, (h_\ell^{-1} - 1)\mathbf{C}_{\ell-1}^{y|x}). \end{aligned} \quad (12)$$

In the linear Gaussian case and large sample limit the above ensemble Kalman move becomes

$$\begin{aligned} x_\ell^{(i)} &= x_{\ell-1}^{(i)} + Q_{\ell-1}H^T \left( (HQ_{\ell-1}H^T + R) + (h_\ell^{-1} - 1)R \right)^{-1} (y - y_{\ell-1}^{(i)} - \eta_\ell^{(i)}), \\ y_{\ell-1}^{(i)} &\sim \mathbf{N}(y_{\ell-1} \mid Hx_{\ell-1}^{(i)}, R), \\ \eta_\ell^{(i)} &\sim \mathbf{N}(\eta_\ell \mid 0, (h_\ell^{-1} - 1)R). \end{aligned}$$

Where the  $(h_\ell^{-1} - 1)$  scaling has been chosen to ensure that

$$\begin{aligned} \mathbb{E}[x_\ell^{(i)}] &= m_{\ell-1} + Q_{\ell-1}H^T (HQ_{\ell-1}H^T + h_\ell^{-1}R)^{-1} (y - Hm_{\ell-1}), \\ \text{Cov}[x_\ell^{(i)}] &= Q_{\ell-1} - Q_{\ell-1}H^T (HQ_{\ell-1}H^T + h_\ell^{-1}R)^{-1} HQ_{\ell-1}. \end{aligned}$$

These limiting statistics coincide with (9) and therefore the ensemble Kalman update in (12) is asymptotically unbiased in the linear Gaussian case, and consistent with the ensemble Kalman paradigm.

---

**Algorithm 1** Ensemble Kalman Inversion for General Likelihoods

---

- 1: Given (possibly adaptive) method to set inverse temperatures  $\lambda_\ell$  and stopping criterion  $L$
- 2: Sample from prior

$$x_0^{(i)} \sim p(x) \quad i = 1, \dots, N$$

3: **for**  $\ell = 1, \dots, L$  **do**

- 4: Simulate observations

$$y_{\ell-1}^{(i)} \sim p(y \mid x_{\ell-1}^{(i)}) \quad i = 1, \dots, N$$

5: Form sample covariances  $C_{\ell-1}^{xx}, C_{\ell-1}^{xy}, C_{\ell-1}^{yy}$  (10) and  $C^{y|x}$  (11).

6: Set stepsize  $h_\ell = \lambda_\ell - \lambda_{\ell-1}$

7: **for**  $i = 1, \dots, N$  **do**

- 8: Generate observation perturbations

$$\eta_\ell^{(i)} \sim \mathcal{N}\left(0, (h_\ell^{-1} - 1) C_{\ell-1}^{y|x}\right)$$

9: Move particles

$$x_\ell^{(i)} = x_{\ell-1}^{(i)} + C_{\ell-1}^{xy} \left( C_{\ell-1}^{yy} + (h_\ell^{-1} - 1) C_{\ell-1}^{y|x} \right)^{-1} \left( y - y_{\ell-1}^{(i)} - \eta_\ell^{(i)} \right)$$

10: **return**  $\{x_L^{(i)}\}_{i=1}^N$

---

### 3.2 Stepsize Selection

The motivation of iterative ensemble Kalman inversion is that for difficult non-Gaussian problems, moving directly from prior to posterior in one step is an extremely difficult task. By taking many smaller steps the particles can explore the state-space and have a better chance of settling in regions of high posterior probability. There is, therefore, a trade-off to be made - more steps means greater exploration but also more likelihood simulations and a longer runtime.

The stepsizes equivalently define an inverse temperature schedule

$$0 = \lambda_0 < \lambda_1 < \dots < \lambda_L$$

where  $h_\ell = \lambda_\ell - \lambda_{\ell-1} > 0$  for  $\ell = 1, \dots, L$ .

In SMC samplers [5] it is common for the next inverse temperature (and therefore stepsize) to be selected adaptively [15] such that the effective sample size (of the sequential importance weights  $\{w_\ell^{(i)}\}_{i=1}^N$ ) decreases by a fixed amount. That is, select  $\lambda_\ell$  such that  $\text{ESS}(\{w_\ell^{(i)}\}_{i=1}^N) \approx \rho N$ , where the normalised weights are a function of  $\lambda_\ell$  and  $\rho \in (0, 1)$  is a tuning parameter that controls the size of the steps. The root for  $\lambda_\ell$  can be found using a bisection algorithm in  $(\lambda_{\ell-1}, \lambda_L]$  and requires no additional likelihood evaluations. This idea was ported to ensemble Kalman inversion in [10] where the following psuedo-weights are used

$$\hat{w}_\ell^{(i)} \propto \exp\left(-\frac{1}{2}(\lambda_\ell - \lambda_{\ell-1}) \left(y - \mathcal{H}(x_{\ell-1}^{(i)})\right)^T R^{-1} \left(y - \mathcal{H}(x_{\ell-1}^{(i)})\right)\right),$$

as ensemble Kalman inversion does not compute importance weights inherently. Here we directly adapt these pseudo-weights to the general likelihood case

$$\hat{w}_\ell^{(i)} \propto \exp\left(-\frac{1}{2}(\lambda_\ell - \lambda_{\ell-1})\left(y - y_{\ell-1}^{(i)}\right)^T C_{\ell-1}^{y|x-1}\left(y - y_{\ell-1}^{(i)}\right)\right). \quad (13)$$

The effective sample size (over true importance weights) can be viewed as a measure of the  $\chi^2$ -divergence between the tempered posterior at  $\lambda_{\ell-1}$  and  $\lambda_\ell$  [4]. In [11] this idea was extended to instead use an effective sample size based on the symmetric KL-divergence.

As noted in [10], the lack of resampling means the user can be more aggressive with the choice of  $\rho$ , in our experiments we set  $\rho = \frac{1}{2}$ .

### 3.3 Stopping Criteria

We consider two stopping criteria:

- **Sampling** - stop when  $\lambda_L = 1$ . This stopping criterion mimics that of tempered likelihood approaches for tractable likelihoods and is applied to ensemble Kalman inversion in [10]. This approach is asymptotically unbiased for the true posterior in the linear Gaussian case and aims to quantify uncertainty around parameters.
- **Optimisation** - stop when the marginal standard deviation (of the particles) in each dimension falls below 0.1 of their initial (prior) standard deviations. Under this approach the algorithm is iterated until the particles form a consensus approaching a single point estimate, which in the linear Gaussian case will (asymptotically) be the maximum likelihood estimator.

## 4 Numerical Experiments

We now examine the performance of both ensemble Kalman inversion for sampling and optimisation versus two approximate Bayesian computation methods for two static Bayesian inference problems with intractable likelihoods.

The first approximate Bayesian computation technique is that of ABC-SMC [6]. In ABC-SMC, a series of importance weighted Monte Carlo approximations are generated iteratively to target

$$\nu_\kappa(x, y') \propto p(x)p(y | x)\mathbb{I}[\|y - y'\| < \kappa], \quad (14)$$

for a series of decreasing threshold parameters  $\kappa_0 > \kappa_1 > \dots > \kappa_L$ . Here  $y$  is the true data and  $y'$  is the simulated data. As described in [5], particles are rejuvenated using a random-walk Metropolis-Hastings kernel, with covariance adapted to  $2.38^2 d_x^{-1} C_{\ell-1}^{xx}$  a scaled version of the empirical covariance of the previous particles and threshold parameters  $\kappa_\ell$  adaptively chosen such that  $\text{ESS} \approx 0.9N$ . Particles are resampled when the ESS drops below  $0.5N$  and the algorithm terminates when the acceptance rate of the Metropolis-Hastings kernel first falls below 1.5%.

We also run the random-walk Metropolis-Hastings kernel directly as an ABC-MCMC algorithm. As described in [23] we use a Robbins-Monro schedule to adaptively tune the stepsize, preconditioner combination to  $2.38^2 d_x^{-1} \hat{\Sigma}$  where  $\hat{\Sigma}$  is the empirical covariance of the historical chain and adapt the threshold parameter  $\kappa$  in (14) such that 10% of samples are accepted.

As mentioned, for EKI we determine the stepsize  $h_\ell$  (equivalently the next inverse temperature  $\lambda_\ell$ ) adaptively such that the ESS of the pseudo-weights (13) is approximately  $0.5N$ . We examine both the sampling and optimisation stopping criteria discussed in Section 3.3.

### 4.1 $g$ -and- $k$ distribution

Popular as a benchmark for ABC algorithms the  $g$ -and- $k$  distribution family is defined by the quantile function

$$F^{-1}(u) = A + B \left(1 + c \frac{1 - \exp(-gz(u))}{1 + \exp(-gz(u))}\right) (1 + z(u)^2)^k z(u), \quad (15)$$

where  $z(\cdot)$  is the quantile function of a standard normal distribution. The constant  $c$  is typically set to 0.8 and considered known. We set the remaining parameters  $x = (A, B, g, k)$  with *true* values  $(3, 1, 2, 1/2)$  but consider them unknown (to be inferred) with prior  $\mathcal{U}(0, 10)^4$ . The  $g$ -and- $k$  likelihood is defined implicitly by the quantile function (15). This likelihood function cannot be evaluated easily and thus we cannot easily utilise traditional posterior inference methods such as MCMC or importance sampling - although their ABC counterparts are

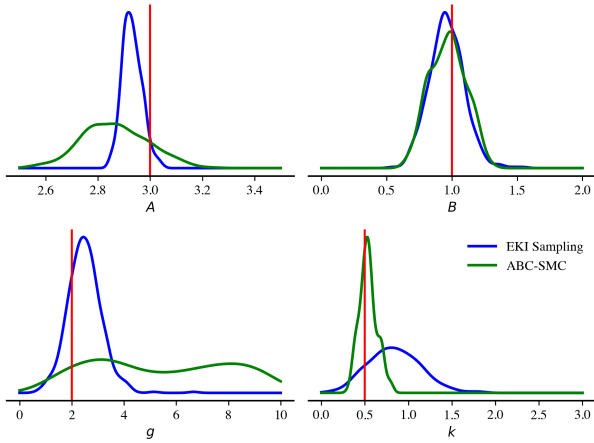


Figure 1: Marginal densities for EKI sampling and ABC-SMC.

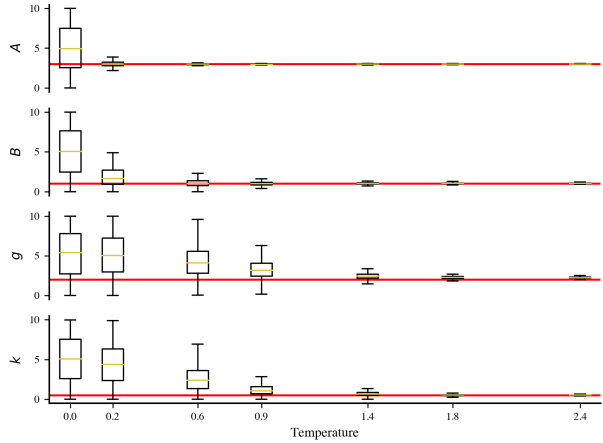


Figure 2: Convergence of EKI for optimisation.

*g*-and-*k* distribution,  $N = 500$ , truth in red.

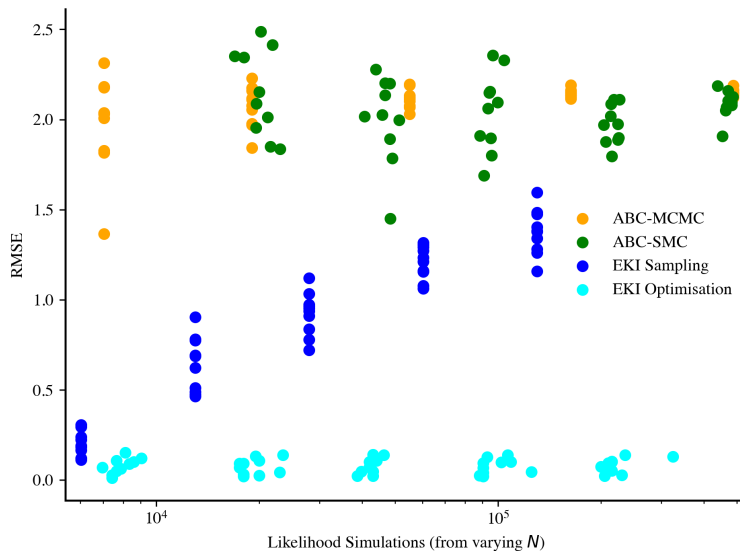


Figure 3: Root mean squared error for number of likelihood simulation induced by varying  $N$ , on *g*-and-*k* distribution. Repeated over 10 randomly generated sets of observations.

still possible as the likelihood can be easily simulated for given parameters by simply evaluating the quantile function at a sampled standard uniform random variable.

We assume we have data of 1000 i.i.d. samples from (15) which we summarise into 100 evenly spaced order statistics for both EKI and ABC. For ABC we use the Euclidean distance function. For both ABC and EKI we unconstrain the parameters using the transformation  $z(\cdot/10)$ .

In Figure 1, we compare the marginal distributions produced by EKI for sampling and those from ABC-SMC. We observe that EKI has centred on the vicinity of the truth for all 4 parameters whereas ABC-SMC has failed to concentrate in the *g* variable in particular. We note that the two posteriors differ quite significantly - an indication of the high levels of non-linearity in the *g*-and-*k* likelihood - yet the EKI posterior remains informative.

We then examine the second EKI stopping criterion, that of optimisation. The EKI optimisation procedure, Section 3.3, iterates beyond  $\lambda_\ell = 1$  until a consensus is reached on a single point approximation for the maximum likelihood estimator. Figure 2 displays 7 equally spaced iterations as the adaptive inverse temperature schedule increases above  $\lambda_\ell = 1$  before terminating when all standard deviations are suitably small. The particles converge quickly and very closely to the true underlying parameter values.

Finally, we vary the sample size  $N$  between 200 and 5000 then repeat the experiment 10 times. We plot the root mean squared error against the number of likelihood simulations utilised by each algorithm as  $N$  changes in Figure 3. We observe that both EKI stopping criteria are consistently outperforming both ABC-MCMC and

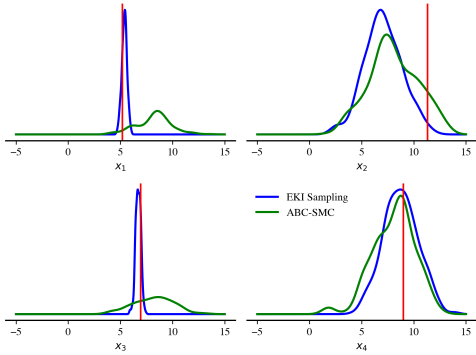


Figure 4: Marginal densities for EKI sampling and ABC-SMC.

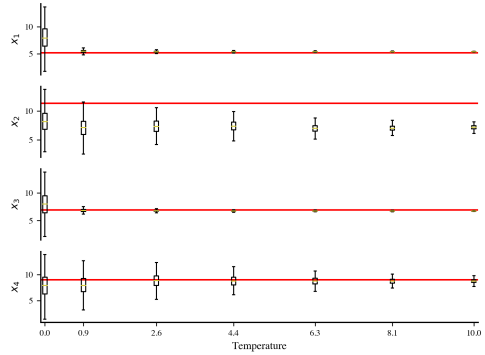


Figure 5: Convergence of EKI for optimisation.

Lorenz 96 example,  $N = 500$ , truth in red.

ABC-SMC for the same computational cost. Curiously, we observe that the performance of EKI for sampling deteriorates as  $N$  increases although this is not the case for the optimisation approach. We posit that this might be due to the smaller sample sizes under estimating the noise covariance (a common occurrence in ensemble Kalman techniques [22]) and therefore moving the particles further.

## 4.2 Stochastic Lorenz 96

We now consider the task of inferring the initial conditions of a noisy version of the Lorenz 96 model [17]. The Lorenz 96 (from 1995) is a simplified model of oceanic flows that is commonly used as a testbed for high-dimensional data assimilation techniques such as the ensemble Kalman filter.

The Lorenz 96 dynamics (with added stochasticity) are defined by the SDE

$$dx_t[m] = -x_t[m-2]x_t[m-1]dt + x_t[m-1]x_t[m+1]dt - x_t[m]dt + Fdt + \omega dW_t,$$

for  $m = 1, \dots, d_x$  with cyclic coordinates  $x_t[0] = x_t[d_x]$ ,  $x_t[-1] = x_t[d_x - 1]$  and  $x_t[d_x + 1] = x_t[1]$ . We adopt the common high-dimensional setup of  $d_x = 40$  and  $F = 8$ , which is known to produce challenging, chaotic dynamics.

We define our inference goal as obtaining the initial conditions  $x_0 \in \mathbb{R}^{d_x}$  given observations of every other dimension, perturbed by Gaussian noise with variance 0.1, at times  $t = 1, 2, 3, 4, 5$  - resulting in  $d_y = 100$  observations. We set the prior to  $p(x_0) = \mathbf{N}(x_0 | F, 5\mathbb{I}_{40})$  and simulate from the likelihood with an Euler-Maruyama scheme (stepsize 0.001). The stochasticity in the Lorenz 96 dynamics provides a more realistic influence of noise but the iterative addition of noise in the Euler-Maruyama scheme makes evaluating the likelihood density intractable.

In our experiments, underlying true values for the initial conditions are sampled from the prior and then observations generated using the same Euler-Maruyama scheme as above.

Recall that odd dimensions are directly observed whereas even dimensions are unobserved. We observe in Figure 4 that EKI for sampling converges very closely around the truth in observed dimensions and is understandably less certain about unobserved dimensions. In contrast ABC-SMC, performs similarly for all dimensions and is likely struggling with the dimensionality of the problem.

When we push the EKI into high inverse temperatures in Figure 5 we first see that the particles struggle to collapse in unobserved dimensions. This is an indication that the given observations are insufficient to provide a confident point estimate in those unobserved dimensions. We also notice that the particles converge in the second dimension away from the true underlying value of the parameter - this may be an indication that the true maximum likelihood is not necessarily guaranteed to be close to the truth under this model setup.

In Figure 6, we also observe the phenomenon of decreasing performance in EKI for sampling as  $N$  increases for the L96 example - although less so. However, again we see that EKI consistently outperforms ABC, although this is perhaps not surprising in a high-dimensional example given the regular use of ensemble Kalman techniques in this type of high-dimensional problem. In this case, the EKI for optimisation utilised significantly more likelihood simulations as it requires more iterations to converge - it also suffered high variance results whereas the performance of the EKI for sampling was more steady.

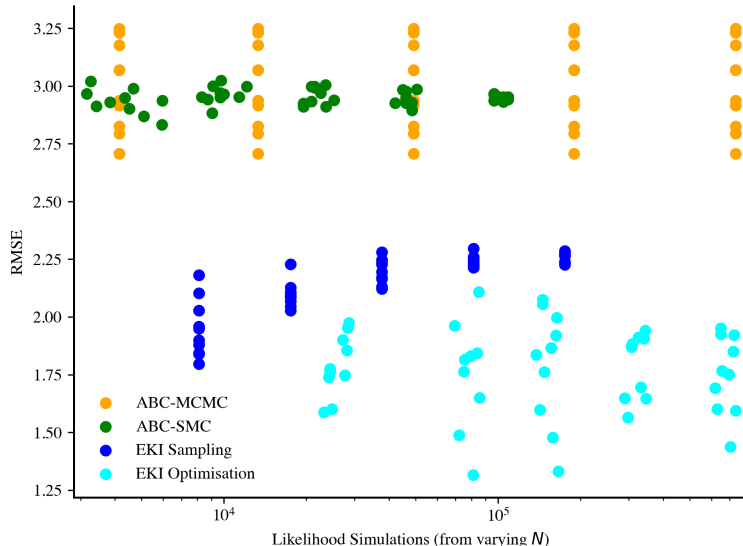


Figure 6: Root mean squared error for number of likelihood simulation induced by varying  $N$ , on Lorenz 96 example. Repeated over 10 randomly generated sets of observations.

## 5 Conclusion

In this letter we have extended the work of ensemble Kalman inversion [13, 10] to problems with general likelihoods as opposed to the common restriction of additive Gaussian noise. We remain faithful to the ensemble Kalman paradigm, i.e. our generalisation remains asymptotically unbiased in the linear Gaussian case. We described how to apply the technique for both optimisation and for sampling or uncertainty quantification. We have demonstrated both speed and accuracy of the novel ensemble Kalman inversion algorithm in a difficult benchmark problem as well as a high dimensional spatial example. The computational cost of the ensemble Kalman inversion is  $O(Ld_x^3 + LN d_x^2)$  and only requires  $LN$  likelihood simulations which is the typical computational bottleneck for problems within approximate Bayesian computation.

We observe the curious phenomenon that increasing the number of particles fails to increase accuracy when applying ensemble Kalman inversion for sampling - at least in terms of mean square error. An outstanding question is how to correct for this. This phenomenon is not entirely new but is not well understood, it would be intriguing to investigate whether it could potentially be mitigated by covariance regularisation [8] or moment-matching ideas [16].

A natural extension of the stochastic ensemble Kalman inversion algorithm presented in this chapter would be the conversion to the square-root ensemble Kalman variants [3, 1] that instead deterministically move particles in a way that remains asymptotically unbiased for fully linear Gaussian problems. By removing a layer of stochasticity we hope to increase the numerical stability of the inversion algorithm.

Outside of linear Gaussian problems, ensemble Kalman inversion is asymptotically biased. It would be interesting to investigate embedding an ensemble Kalman kernel within an ABC-SMC sampler. This way, the ensemble Kalman inversion would inherit the theory of approximate Bayesian computation and become asymptotically unbiased for  $\nu_\kappa$ . However, it is not clear how to choose the backward kernel to induce stable importance weights.

A further application of the presented ensemble Kalman inversion would be to investigate its use within state-space models. It may be that utilising an iterative tempered approach to the update step within an ensemble Kalman filter may improve sample quality. Additionally, we could adapt ensemble Kalman inversion to be used in the online setting of state-space models with intractable observation densities [14].

## References

- [1] Jeffrey L. Anderson. An Ensemble Adjustment Kalman Filter for Data Assimilation. *Monthly Weather Review*, 129(12):2884 – 2903, 2001.
- [2] Mark A. Beaumont. Approximate Bayesian Computation. *Annual Review of Statistics and Its Application*, 6(1):379–403, 2019.
- [3] Craig H. Bishop, Brian J. Etherton, and Sharanya J. Majumdar. Adaptive Sampling with the Ensemble Transform Kalman Filter. Part I: Theoretical Aspects. *Monthly Weather Review*, 129(3):420 – 436, 2001.

- [4] Nicolas Chopin and Omiros Papaspiliopoulos. *Introduction to Sequential Monte Carlo*. Springer International Publishing, 2020.
- [5] Pierre Del Moral, Arnaud Doucet, and Ajay Jasra. Sequential Monte Carlo Samplers. *Journal of the Royal Statistical Society. Series B (Statistical Methodology)*, 68(3):411–436, 2006.
- [6] Pierre Del Moral, Arnaud Doucet, and Ajay Jasra. An Adaptive Sequential Monte Carlo method for Approximate Bayesian Computation. *Statistics and Computing*, 22(5):1009–1020, Sep 2012.
- [7] Geir Evensen. Sequential Data Assimilation with a Nonlinear Quasi-geostrophic Model using Monte Carlo Methods to Forecast Error Statistics. *Journal of Geophysical Research: Oceans*, 99(C5):10143–10162, 1994.
- [8] P. L. Houtekamer and Herschel L. Mitchell. A Sequential Ensemble Kalman Filter for Atmospheric Data Assimilation. *Monthly Weather Review*, 129(1):123 – 137, 2001.
- [9] P. L. Houtekamer, Herschel L. Mitchell, Gérard Pellerin, Mark Buehner, Martin Charron, Lubos Spacek, and Bjarne Hansen. Atmospheric Data Assimilation with an Ensemble Kalman Filter: Results with Real Observations. *Monthly Weather Review*, 133(3):604 – 620, 2005.
- [10] Marco Iglesias, Minhho Park, and M V Tretyakov. Bayesian Inversion in Resin Transfer Molding. *Inverse Problems*, 34(10):105002, jul 2018.
- [11] Marco Iglesias and Yuchen Yang. Adaptive Regularisation for Ensemble Kalman Inversion, 2020.
- [12] Marco A. Iglesias. Iterative Regularization for Ensemble Data Assimilation in Reservoir Models. *Computational Geosciences*, 19(1):177–212, Feb 2015.
- [13] Marco A Iglesias, Kody J H Law, and Andrew M Stuart. Ensemble Kalman Methods for Inverse Problems. *Inverse Problems*, 29(4):045001, mar 2013.
- [14] Ajay Jasra, Sumeetpal S. Singh, James S. Martin, and Emma McCoy. Filtering via Approximate Bayesian Computation. *Statistics and Computing*, 22(6):1223–1237, Nov 2012.
- [15] Ajay Jasra, David A. Stephens, Arnaud Doucet, and Theodoros Tsagaris. Inference for Lévy-Driven Stochastic Volatility Models via Adaptive Sequential Monte Carlo. *Scandinavian Journal of Statistics*, 38(1):1–22, 2011.
- [16] Jing Lei and P. Bickel. A Moment Matching Ensemble Filter for Nonlinear Non-Gaussian Data Assimilation. *Monthly Weather Review*, 139:3964–3973, 2011.
- [17] E.N. Lorenz. Predictability: A Problem Partly Solved. In *Seminar on Predictability, 4-8 September 1995*, volume 1, pages 1–18, Shinfield Park, Reading, 1995. ECMWF, ECMWF.
- [18] Andrew J. Majda and Xin T. Tong. Performance of ensemble kalman filters in large dimensions, 2017.
- [19] Patrick Rebeschini and Ramon van Handel. Can Local Particle Filters beat the Curse of Dimensionality? *The Annals of Applied Probability*, 25(5):2809 – 2866, 2015.
- [20] Michael Roth, Gustaf Hendeby, Carsten Fritsche, and Fredrik Gustafsson. The Ensemble Kalman Filter: A Signal Processing Perspective. *EURASIP Journal on Advances in Signal Processing*, 2017(1):56, Aug 2017.
- [21] Claudia Schillings and Andrew Stuart. Analysis of the Ensemble Kalman Filter for Inverse Problems. *SIAM Journal on Numerical Analysis*, 55, 02 2016.
- [22] Xin T Tong, Andrew J Majda, and David Kelly. Nonlinear stability and ergodicity of ensemble based kalman filters. *Nonlinearity*, 29(2):657–691, jan 2016.
- [23] Matti Vihola and Jordan Franks. On the Use of Approximate Bayesian Computation Markov Chain Monte Carlo with Inflated Tolerance and Post-correction. *Biometrika*, 107(2):381–395, 02 2020.